T. Inoue, T. Hoshide,* and E. Kakiuchi**

Fatigue Life Evaluation of Notched Components under Combined Axial–Torsional Loading

REFERENCE Inoue, T., Hoshide, T., and Kakiuchi, E., **Fatigue life evaluation of notched components under combined axial-torsional loading**, *Multiaxial Fatigue and Design*, ESIS 21 (Edited by A. Pineau, G. Cailletaud, and T. C. Lindley) 1996, Mechanical Engineering Publications, London, pp. 301–313.

ABSTRACT A procedure to evaluate the subsequent life after an initial fatigue stage, specified by a distribution of small cracks, was proposed for a notched component subjected to cyclic combined axial–torsional loading. Distributed cracks at the initial stage were modelled as straight-line cracks by using an image-processing technique. The algorithm for the analysis of crack growth after the initial stage was constructed by taking account of both modes of the propagation as a single crack and the coalescence between propagating cracks. Fatigue tests under combined axial–torsional loading with constant and variable amplitudes were conducted using cylindrical specimens with circumferential blunt notches. The dependence of fatigue life and cracking morphology on loading pattern was clarified experimentally. When compared with the same value of the equivalent plastic strain range, the fatigue life became longer with increasing shear components in the stress state, with no significant difference between two loading patterns of constant and variable stress amplitudes. The fatigue life defined by the formation of cracks with a specific length was evaluated based on the proposed procedure. The predicted life almost coincided with the experimental data. Cracking morphology was also simulated by using the present model to show good agreement with that observed experimentally.

1 Introduction

When the coalescence between small cracks is one of typical cracking morphologies, the fatigue life is found to be reduced significantly, compared with that predicted by the propagation mode of a single crack (**1–4**).

The authors (**2, 3**) have proposed a procedure to evaluate failure life by taking account of the coalescence between modelled cracks in a specified initial stage during push-pull fatigue process of smooth specimens. It is anticipated, however, that the cracking behaviour in notched components subject to combined loading, which is more important in fatigue design, is different from that under uniaxial stress state. More suitable procedures to estimate failure life under complex stress states should be developed by adequately modelling the cracking

*Department of Energy Science and Engineering, Kyoto University, Yoshida-honmachi, Sakyo-ku, Kyoto 606-01, Japan.

behaviour affected by the stress state. An automatic method of crack identification is also required in modelling of small cracks, because it is tedious to deal with many cracks observed on specimen surfaces.

In this study, an analytical procedure to evaluate failure life under cyclic combined loading was developed for a specified initial state of distributed small cracks. An image-processing technique was used as a methodology to identify small cracks automatically. Distributed cracks at the initial stage were modelled as straight-line cracks by using the image-processing technique. Fatigue tests under combined axial–torsional loading were also conducted for cylindrical specimens with circumferential blunt notches of pure copper and a medium carbon steel. A computer simulation based on the proposed procedure was carried out to compare the analytical results with experimental observations in the failure life and cracking morphology.

2 Modelling of Distributed Cracks

Micrographs of replicas taken from the specimen surface were employed in the analysis. Through an image-scanner, images of regions including distributed small cracks on photographs were processed into digital data using a personal computer, where commerical software of image-processing (**5**) was used. The region to be analysed was the same region, including the largest crack with a total length of 6 or 7 times the mean grain size of the material, as where the dominant crack was formed in the succeeding fatigue process. Cracks on micrographs were identified from other images by a threshold operation. The crack image obtained by the operation was further processed by a skeleton mask. This process reduced the crack image to the curved line with one pixel in width. After the process, the coordinates of the starting and end points of the processed crack image were obtained by tracing the crack line from tip to tip. Finally, the crack was modelled as the straight line connecting the starting and end points, although observed cracks were often wavy in some materials. Cracks to be analysed were limited to those with the length larger than the mean grain size.

3 Procedure to Evaluate Failure Life

3.1 *Primitive procedure to evaluate propagation life of single crack*

In the evaluation of crack propagation life, we considered a propagation of single semi-elliptical surface crack with a surface length of $2a$ and an aspect ratio λ, defined as the ratio of the depth to the half length on the surface. The crack propagation life is analysed assuming that the growth rate da/dN is described by a power function of the range of J-integral ΔJ such that

$$da/dN = C(\Delta J)^m \tag{1}$$

The J-integral range ΔJ for the mode I crack is evaluated by equation (6).

$$\Delta J = 2\pi M_J \Delta W a \tag{2}$$

where $M_J = (M_K/\Phi)^2\lambda$, and M_K is the geometric correction factor for the stress intensity factor of the crack under consideration and Φ is the complete elliptic integral of the second kind. The energy density parameter ΔW is given as

$$\Delta W = \Delta\sigma^2/(2E) + f_1(n')\Delta\sigma\Delta\varepsilon^p/(1 + n') \tag{3}$$

with

$$f_1(n') = (1 + n')[3.85(1 - n')n'^{-1/2} + \pi n']/(2\pi) \tag{4}$$

where E and n' are the Young's modulus and the exponent of cyclic strain hardening, respectively. As for the mode II crack, M_J should be replaced by the square of the magnification factor (7) and ΔW is calculated as follows (8)

$$\Delta W = \Delta\tau^2(1 + \nu)/(E) + f_2(n')\Delta\bar{\sigma}\Delta\bar{\varepsilon}^p/(1 + n') \tag{5}$$

with

$$f_2(n') = (1 + n')[1.45(1 - n')n'^{-1/2} + \pi n'/(2 + 2\nu)]/(2\pi) \tag{6}$$

where ν is the Poisson's ratio. In equations (3) and (5), the ranges of nominal stress and nominal plastic strain at the notch root in one loading cycle, which are evaluated by an elastoplastic finite-element analysis, are used and barred parameters represent the equivalent stress and strain ranges. In the case of constant stress amplitude, the number of cycles ΔN required for a given extension, Δa, from half crack length a can be evaluated by integrating equation (1) with respect to the crack length as

$$\Delta N = [a^{1-m} - (a + \Delta a)^{1-m}]/[A(\Delta W)^m] \tag{7}$$

where

$$A = C(m - 1)(2\pi M_J)^m \tag{8}$$

The formulation mentioned above is developed for the case of variable stress amplitude as follows. Consider k kinds of different stress amplitudes in one block loading. The number of cycles of the ith stress amplitude is denoted as n_i, and the energy density parameters during the ith stress amplitude cycling as ΔW_i. By replacing ΔN with n_i and also ΔW with ΔW_i in equation (7) and taking summation with respect to i, we have the relation

$$\Sigma[n_i(\Delta W_i)^m] = [a^{1-m} - (a + \Sigma\Delta a_i)^{1-m}]/A \tag{9}$$

where Δa_i is a crack increment after n_i cycles of ith stress amplitude. By defining the equivalent energy density parameter ΔW_{eq} as

$$(\Delta W_{eq})^m = \Sigma[n_i(\Delta W_i)^m]/(\Sigma n_i) \tag{10}$$

a more generalized equation instead of equation (7) is obtained as follows

$$\Delta N = [a^{1-m} - (a + \Delta a)^{1-m}]/[A(\Delta W_{eq})^m] \tag{11}$$

where $\Delta N = \Sigma n_i$ and $\Delta a = \Sigma \Delta a_i$. Summations in the above equations are taken with respect to i.

3.2 *Life evaluation by taking account of crack coalescence*

The number of stress cycles, at which the largest crack with 6 or 7 times the mean grain size in total length is detected at the region, is defined as an initial stage. The crack coalescence analysis is made during the propagation process after the initial stage. On the basis of the experimental observations (**9,10**), the crack is assumed to propagate perpendicularly to the direction of the maximum principal stress, except for the case when the crack propagates in the direction of the maximum shear stress. In the exceptional situation, it is reasonable to postulate that the crack propagates in the direction parallel to the maximum shear stress. Consider the Cartesian coordinate x–y such that the circumferential direction coincides with x-axis and the axial direction with y-axis. By rotating the original coordinate, another Cartesian coordinate x'-y' is introduced such that the x'-axis is parallel to the assumed direction of crack growth (see Fig. 1).

The coalescence is assumed to occur when the difference $\Delta x'_{ij}$ in the x' direction between the tips of the ith and jth cracks as shown in Fig. 1(a) becomes zero. For this criterion, the additional condition is imposed such that the difference $\Delta y'_{ij}$ in the y' direction between the crack tips as shown in Fig. 1(b) is less than δ_c. The parameter δ_c is supposed to depend on the microstrucuture of material and the lengths of cracks to be linked. If the coalescence criterion is satisfied for two cracks, the linked cracks will be treated as the single straight-line crack in the subsequent analysis. For the cycle increment ΔN from a specified number of cycles, equation (11) is employed to check the criterion for $\Delta x'_{ij}$ such as

$$\Delta x'_{ij} = (x'^{L}_j - \Delta a_j) - (x'^{R}_i + \Delta a_i) \tag{12}$$

where Δa_i and Δa_j are the crack increments for the ith and jth cracks, respectively. By checking the coalescence criterion for each iteration cycle, the residual life of a component with a given initial distribution of small cracks will be evaluated by using equation (11) in the calculation of the cycles required for the formation of cracks with a specified length.

4 Fatigue Tests of Notched Specimens

4.1 *Materials and specimen*

Materials used in this experiment were an oxygen-free pure copper with purity of 99.98% including 6 ppm of oxygen (JIS C1020) and a medium carbon steel with 0.37 wt%C (JIS S35C). The specimen was of solid cylindrical type with a circumferential blunt notch as illustrated in Fig. 2. Specimens with a notch root

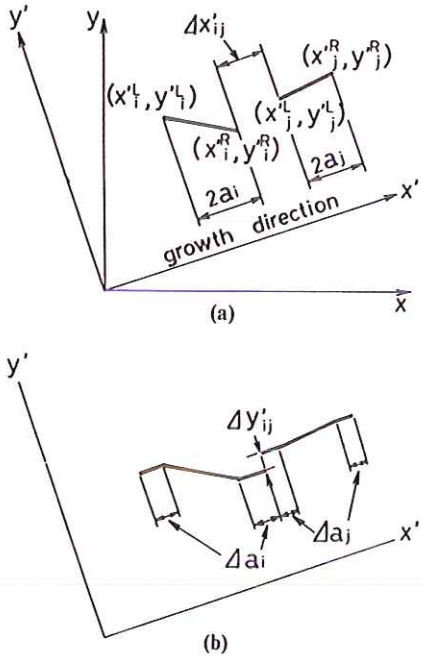

Fig 1 Rotation of coordinates and configuration of modelled cracks.

radius R of 3 mm or 5 mm were prepared. The elastic stress concentration factor for the specimen with $R = 5$ mm is 1.55 under tension and 1.22 under torsion, and that for the specimen with $R = 3$ mm is 1.83 under tension and 1.32 under torsion. Machined specimens were heat treated at 650°C for one hour in vacuum for copper, and 900°C for four hours in vacuum for the steel, followed by cooling in the furnace for both materials. The mean grain size d after the heat treatment was 55 μm for copper and 21 μm for the steel. The steel has the microstructure with a ferrite–pearlite phase, where pearlite grains align along the axial direction of the specimen.

4.2 *Testing procedure*

Fully reversed fatigue tests were conducted under load-controlled conditions with a frequency of 0.4 Hz. Three loading modes of axial, torsional and combined axial–torsional types were investigated in fatigue tests. The load in each mode was controlled so that the range of equivalent stress was constant. According to the deformation behaviour of the material, the equivalent stress of Tresca type for copper and of von Mises type for the steel was used as the controlled stress, respectively. Apparent nominal and shear stresses at the notch root, which

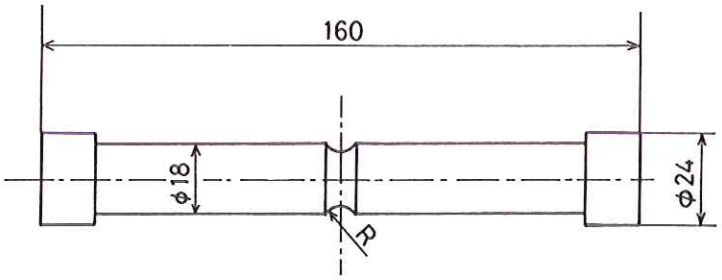

Fig 2 Shape of specimen with notch of root radius R (dimensions are in mm.)

were calculated by using the elastic stress concentration factor, were employed in the evaluation of the controlled equivalent stress. In the following, the loads corresponding to the high and low equivalent stress levels are designated as the high and low load levels, respectively. For copper, the high and low load levels were set as 465 MPa and 388 MPa in the stress range, respectively. Variable stress amplitude tests using copper were also carried out to clarify the applicability of the proposed procedure to the case of more complicated loading. Two types of loading sequence were investigated; one was 10 cycles of high stress level after 100 cycles of low stress level in a block loading, and another was the inverse repetition. For the steel, although the stress range of 1200 MPa was adopted as the high load level in all loading modes, the low level was set as 1100 MPa in the torsional mode and 1000 MPa in the other two modes.

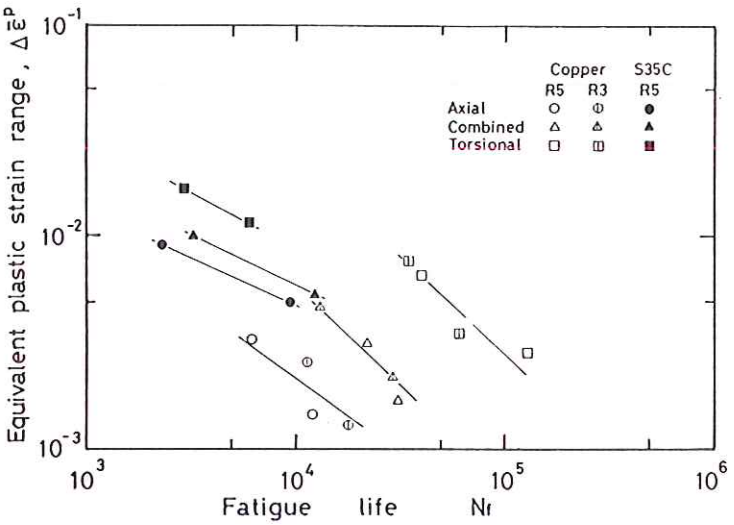

Fig 3 Correlation of fatigue life with equivalent plastic strain in constant stress amplitude tests of copper and steel.

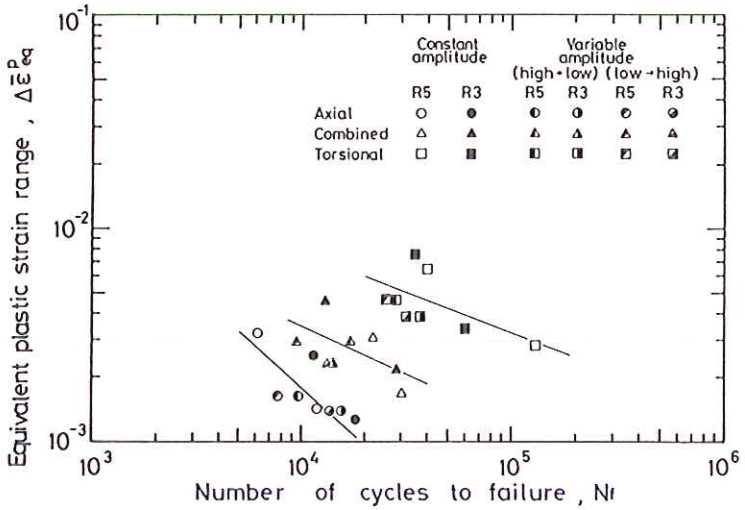

Fig 4 Correlation of fatigue life with equivalent plastic strain in constant and variable stress amplitude tests of copper.

4.3 *Fatigue life characteristics and cracking behaviour*

The strain state at the notch root was calculated by the elastoplastic finite-element method. The relation between the range of equivalent plastic strain $\Delta\bar{\varepsilon}^p_{eq}$ and the fatigue life N_f is shown in Fig. 3. The equivalent strain was evaluated based on the modified von Mises criterion (**11**) for copper and the von Mises criterion for the steel. For both materials, compared for the same equivalent plastic strain, the fatigue life becomes longer as an increasing torsional component was applied to a specimen. This tendency is found to be more significant for copper than for the steel. As for copper, no significant difference between the results for different notch root radii was found for the same loading mode.

On the basis of the linear damage accumulation model using the Coffin–Manson relationship, an equivalent plastic strain range $\Delta\bar{\varepsilon}^p_{eq}$ was defined in the case of variable stress amplitude as

$$\Delta\bar{\varepsilon}^p_{eq} = \{[\Sigma n_i(\Delta\bar{\varepsilon}^p_i)]^\alpha/(\Sigma n_i)\}^{1/\alpha} \tag{13}$$

where α is the power in the Coffin–Manson relation, $(\Delta\varepsilon^p)^\alpha N_f$ = constant, and $\Delta\bar{\varepsilon}^p_i$ is the ith equivalent plastic strain range repeated by n_i cycles during one block loading. Fatigue life in cases of constant and variable stress amplitude tests of copper was correlated with $\Delta\bar{\varepsilon}^p_{eq}$ in Fig. 4. There was no significant variation between the results in both tests, although a similar dependence on loading mode as in constant stress amplitude test was found.

The behaviour of fatigue crack growth was observed by employing a plastic replication technique. Intergranular cracking was observed in copper, while the transgranular type was dominant in the steel. In both materials, the main morphology of crack growth was found to be the coalescence between distributed small cracks. The cracking morphology was dependent on the stress state. The dominant crack propagated in the circumferential direction for the axial loading, and in the direction perpendicular to the maximum principal stress and/or in the circumferential direction for the combined loading. For the torsional loading, however, the crack growth in the direction along the axis of specimen was often observed, although the growth along the axis ceased around 1.5 to 2 mm in crack length. Such a tendency in the torsional situation was more remarkable in the steel than in copper, whence the mode II propagation was predominant in the steel.

5 Analytical Results and Comparison with Experimental Data

5.1 *Parameters used in simulation*

Material parameters in equation (1) for the mode I growth were $C = 4.18 \times 10^{-13}$ and $m = 1.69$ in copper (**12**), and $C = 1.61 \times 10^{-13}$ and $m = 1.68$ in the steel (**1**), when da/dN is presented in m/cycle and ΔJ in N/m. For the mode II growth observed in the steel, parameters in equation (1) were identified by measuring the growth of small cracks without coalescence, and resulted in $C = 1.00 \times 10^{-9}$ and $m = 0.594$. Parameters related to the evaluation of ΔJ are as follows. No variation of the aspect ratio λ was assumed during the fatigue process. In the simulation, two extreme values λ of 0.8 and 1.0 were adopted in accordance with the experimental observation (**1**). Since cracks were assumed to propagate along the x' direction set on the notch root as shown in Fig. 1, the ranges of nominal stress $\Delta\sigma$ and nominal plastic strain $\Delta\varepsilon^p$ calculated through the stress–strain state in the y' direction were used to evaluate ΔW for the cases excluding the steel under torsional loading. In the case of the steel under torsion, the ranges of shear stress $\Delta\tau$ and shear plastic strain $\Delta\gamma^p$ were employed as well as $\Delta\sigma$ and $\Delta\varepsilon^p$, the detail of which is described elsewhere (**8**). The parameter δ_c related to the crack coalescence was postulated to be a function of the mean grain size d and of the half-lengths a_i and a_j of cracks to be linked as follows.

$$\delta_c = 2d + 0.05\,(a_i + a_j) \tag{14}$$

The above relation was determined in order to reflect the experimental result (**2**).

5.2 *Simulation and comparison*

The failure life N_c is defined as the number of cycles required for the formation of the dominant crack with 2.0 mm in the total length for the axial and combined

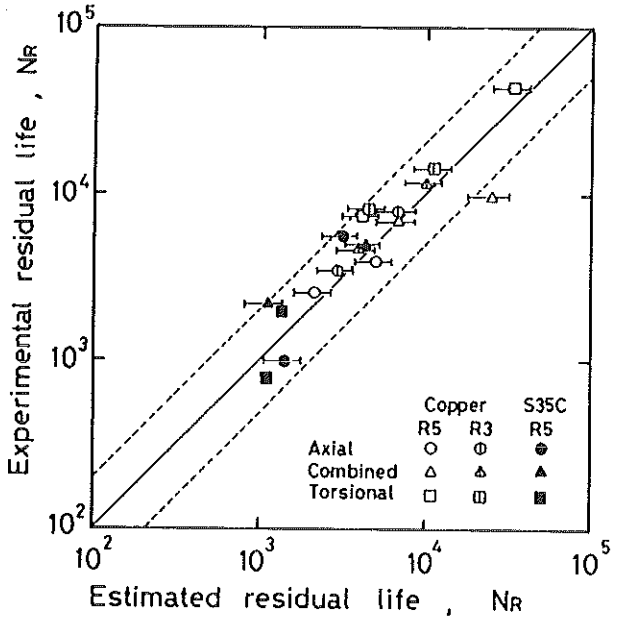

Fig 5 Comparison of estimated residual life with experimental results in constant stress amplitude tests of copper and steel.

loading modes, and the crack with 1.0 mm in the length projected on the axis of specimen for the torsional mode. The residual life N_R is calculated as

$$N_R = N_c - N_i \tag{15}$$

where N_i is the number of cycles at the initial stage, the starting point in the calculation of the residual life.

Figures 5 and 6 indicate the comparison of analytical results with experimental data. The results obtained on copper and on the steel under constant stress amplitude tests are shown in Fig. 5, and Fig. 6 indicates the results obtained from constant and variable stress amplitude tests on copper. The evaluated life in each case is presented with the segment bounded by the two extreme lives which were given as the lower life calculated for the aspect ratio $\lambda = 1.0$ and the higher life for $\lambda = 0.8$, respectively. The mark plotted on the segment for each loading case represents the mean value of the two extreme lives. It is found, however, that the magnification factors of a stress intensity factor for $\lambda = 1.0$ and $\lambda = 0.8$ are almost the same for the mode II cracks (7). Consequently, the residual life in the torsional case for the steel was estimated using M_J calculated from the average of the magnification factors for the two aspect ratios. The broken lines in Figs 5 and 6 present the range of the factor of two. For all situations examined in this study, the analytical results almost coincide with the experimental results within the factor of two.

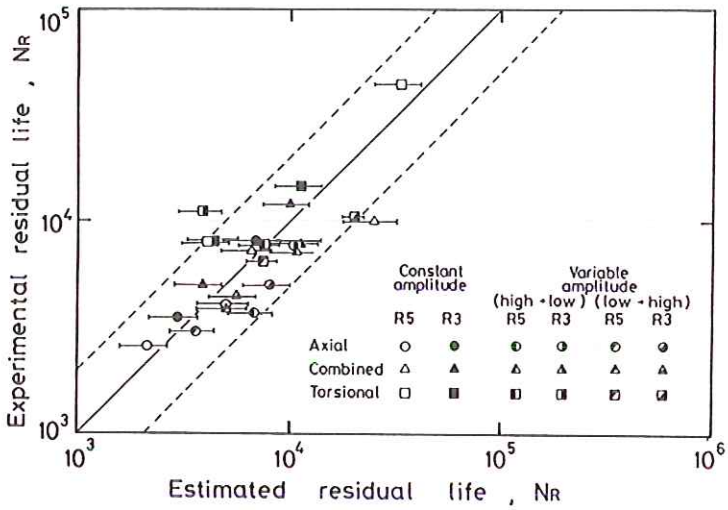

Fig 6 Comparison of estimated residual life with experimental results in constant and variable stress amplitude tests of copper.

It is suggested from the reasonable prediction shown in Figs 5 and 6 that the energy density parameter, which is a dominant parameter in the prediction, may be effective in the correlation with the fatigue life. Figures 7 and 8 present the relation between the fatigue life N_f and ΔW or ΔW_{eq}. The scatter depending

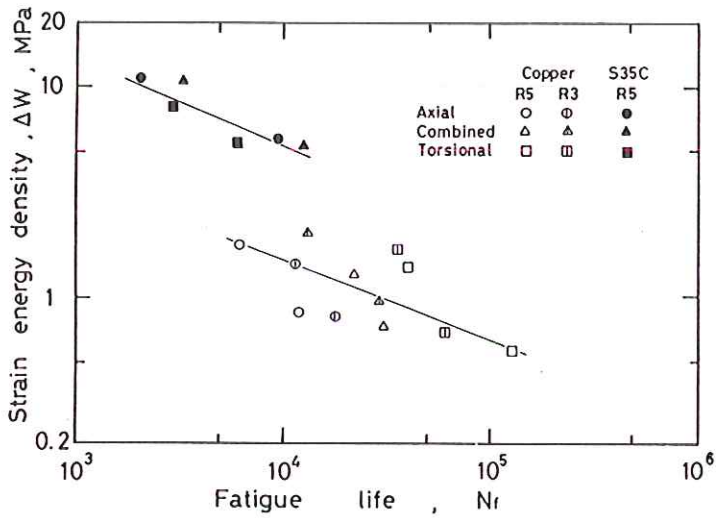

Fig 7 Correlation of fatigue life with strain energy density parameter in constant stress amplitude tests of copper and steel.

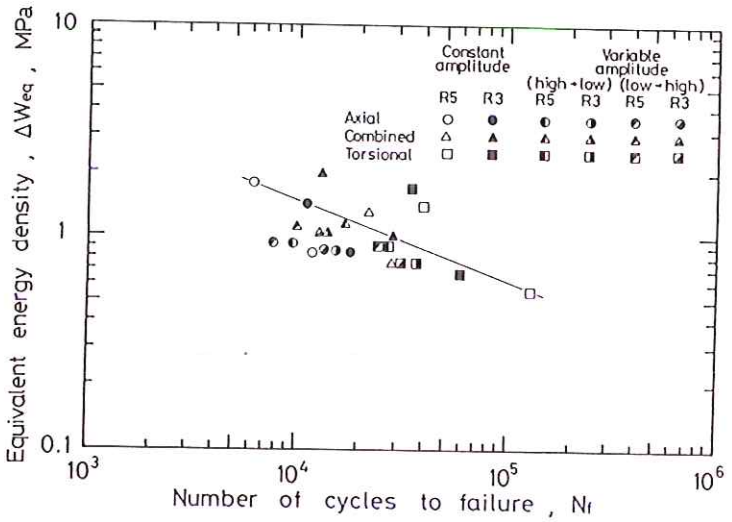

Fig 8 Correlation of fatigue lifetime with strain energy density parameter in constant and variable stress amplitude tests of copper.

on the loading mode is found to be smaller in Figs 7 and 8 than in the correlation with the equivalent plastic strain depicted in Figs 3 and 4.

5.3 *Cracking morphology*

Examples of distributed cracks modelled by the image processing and the crack distribution at the final stage are shown in Figs 9 and 10. Figure 9 illustrates the results in the case of the low stress level for the specimen with $R = 3$ mm in copper, whereas Fig. 10 corresponds to the case of the high level for the specimen with $R = 5$ mm in the steel. For both cases, figures (a) and (b) in each loading mode correspond to the states of crack distribution in the initial and final states, respectively. The feature of the cracking pattern and its dependence on the stress state, which was observed in experiments, is adequately simulated by using the proposed procedure.

6 Conclusions

In the present paper, a procedure to evaluate the residual life under cyclic combined loadings was established for a given initial state of distributed fatigue small cracks. Distributed cracks at the initial stage were modelled as straight line cracks by applying an image processing technique. The algorithm for analysis of the crack growth after the initial stage was constructed by taking account of both modes of the propagation as a single crack and the coalescence between propagating cracks. Fatigue tests under combined axial–torsional loadings were also conducted using cylindrical specimens of pure copper and

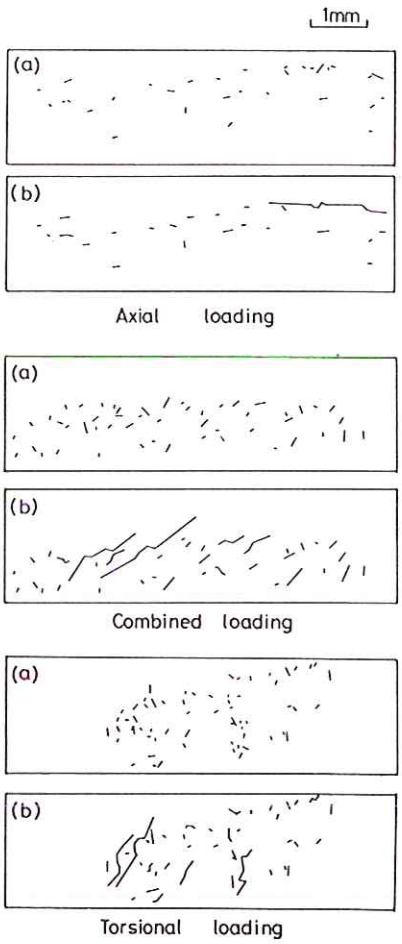

Fig 9 Initial state of image-processed distributed cracks (a) and simulated crack distribution at failure life (b) in copper.

a medium carbon steel with circumferential blunt notches. The fatigue life was correlated with the range of equivalent plastic strain. Compared to the same value of the parameter, the fatigue life became longer with increasing shear component in the stress state at the notch root for both cases of constant and variable stress amplitude tests. The residual life defined by the formation of a crack with a specified length was evaluated by using the proposed procedure. The predicted life was found to coincide with experimental data within a factor of two. Cracking morphology was also simulated on the basis of the present modelling and found to show good correspondence with experimental observation.

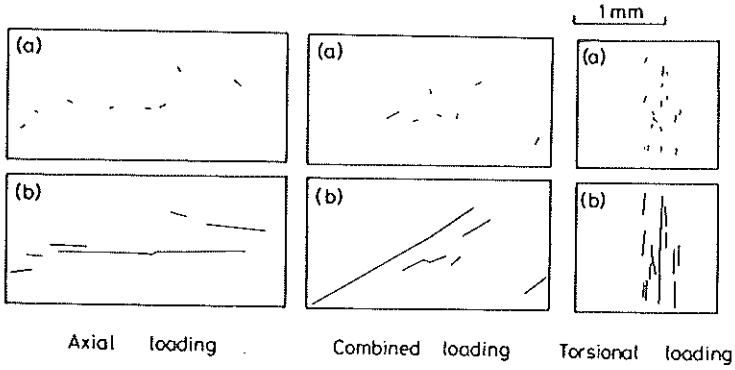

Fig 10 Initial state of image-processed distributed cracks (a) and simulated crack distribution at failure life (b) in steel.

References

(1) HOSHIDE, T., YAMADA, T., FUJIMURA, S. and HAYASHI, T. (1985) Short crack growth and life prediction in low-cycle fatigue of smooth specimens, *Engng. Fracture Mech.*, **21**, p. 85.
(2) HOSHIDE, T., MIYAHARA, M., SATO, M. and INOUE, T. (1986) A life prediction method based on an analysis of crack coalescence in low-cycle fatigue of a smooth specimen, *Trans. Japan Soc. Mech. Engnr, Ser.A*, **52**, p. 406.
(3) HOSHIDE, T., MIYAHARA, M. and INOUE, T. (1987) Life prediction based on analysis of crack coalescence in low-cycle fatigue, *Engng. Fracture Mech.*, **27**, p. 91.
(4) HOSHIDE, T., MIYAHARA, M. and INOUE, T. (1988) Elastic-plastic behaviour of short fatigue crack in smooth specimen, *ASTM STP 924*, **I**, p. 312.
(5) MORIMOTO, Y. (1988) *PIMPOM (Program of Image Processing on Microcomputer)*, Kyoritsu Shupan, Tokyo.
(6) YAMADA, T., HOSHIDE, T., FUJIMURA, S. and MANABE, M. (1983) Life evaluation based on propagation of surface crack in low-cycle fatigue on medium carbon steel, *Trans. Japan Soc. Mech. Engnr, Ser.A*, **49**, p. 441.
(7) SOCIE, D. F., HUA, C. T. and WORTHEM, D. W. (1987) Mixed mode small crack growth, *Fatigue Fracture Engng. Mater. Struct.*, **10**, p. 1.
(8) HOSHIDE, T. and SOCIE, D. F. (1987) Mechanics of mixed mode small fatigue crack growth, *Engng. Fracture Mech.*, **26**, p. 841.
(9) HOSHIDE, T., YOKOTA, K. and INOUE, T. (1990) Investigation on small crack growth and life property in fatigue of circumferentially notched component of pure copper subjected to combined loading, *J. Soc. Mater. Sci., Japan*, **39**, p. 144.
(10) HOSHIDE, T., OGAKI, T, YOKOTA, K. and INOUE, T. (1989) Growth behaviour of small cracks and life properties in fatigue of circumferentially notched specimen subjected to combined loading, *Preprints of 67th Meeting of Japan Soc. Mech. Engnr.*, 18.
(11) YOKOTA, K. (1989) Experimental and analytical approach to crack growth behaviour and life characteristics in low-cycle fatigue of circumferentially notched components subjected to combined axial–torsional loading, master thesis, Kyoto University.
(12) HOSHIDE, T., KAWABATA, K., YAMAKAWA, N. and INOUE, T. (1989) Propagation behaviour of elastic-plastic fatigue crack under biaxial stress state, *J. Soc. Mater. Sci., Japan*, **38**, p. 280.